The Effect of PLC-Inhibitor on Echovirus 1 Internalization Probed with Fluorescently Labeled Echovirus 1

Mira Myllynen

Master's Thesis

University of Jyväskylä

Department of Biological and Environmental Scinece

August 2014

Preface

I had a great opportunity to carry out this Master's Thesis with my supervisors Varpu Marjomäki and Artur Kazmertsuk, who I would both like to thank for encouraging and knowledgeable guidance. It has been a pleasure working with you and learning so much during my Master's thesis work. A combination of Varpu's cheerful and inspiring attitude and Artur's commited and careful way of working, gave me an enjoyable as well as supportive environment to carry out this thesis.

I would also like to thank all the other members of our group for a great and helpful working atmosphere: Ganna Galitska, Anni Honkimaa, Moona Huttunen, Mari Martikainen, Lassi Paavolainen, Maria Pelliccia, Marie Stark and Paula Turkki.

Jyväskylän yliopisto **Pro gradu –tutkielman tiivistelmä**

Matemaattis-luonnontieteellinen tiedekunta

Tekijä: Mira Myllynen

Tutkielman nimi: PLC-inhibiittorin vaikutus echovirus 1:n sisäänmenoon käyttäen fluoresoivasti leimattua echovirus 1:stä

English title: The Effect of PLC-Inhibitor on Echovirus 1 Internalization Probed with Fluorescently Labeled Echovirus 1

Päivämäärä: 14.8.2014 **Sivumäärä:** 42 + 4

Laitos: Bio- ja ympäristötieteiden laitos

Oppiaine: Solu- ja molekyylibiologia

Tutkielman ohjaaja(t): Varpu Marjomäki , Artur Kazmertsuk

Tiivistelmä:

Echovirus 1 (EV1) kuuluu Pikornavirusperheeseen ja tarkemmin luokiteltuna Enterovirusten sukuun. EV1 on pieni ja vaipaton RNA-virus, jonka proteiinikuori koostuu neljästä proteiinista VP1-VP4. Infektion on osoitettu alkavan, kun EV1 tarttuu $\alpha_2\beta_1$-integriiniin solun pinnalla, jonka jälkeen virus otetaan solun sisään kaveoliinivälitteistä endosytoosia sekä makropinosytoosia muistuttavalla mekanismilla. Toisaalta sitä, kuinka virus avautuu sekä vapauttaa RNA:nsa, ei vielä tarkalleen tiedetä. Tässä tutkimuksessa EV1 puhdistettiin ensin sakkaroosigradientilla, jonka jälkeen virus leimattiin fluoresoivalla amiinireaktiivisella värillä. Tulokset osoittivat, että leimauksen onnistumiseksi tarvitaan suhteellisen vähäinen leimamäärä, ja että vähäinen leimamäärä riittää fluoresenssin havaitsemiseksi sekä on tärkeä viruksen infektiivisyyden säilyttämiseksi. Leimattua EV1:stä käytettiin solukokeissa, joissa Fosfolipaasi C inhibiittoria (PLC-inhibiittori) käytettiin viruksen endosytoosin estämiseen, jolloin asettamamme hypoteesin mukaan endosytoosia ei tapahdu, vaan virus jää solun pinnalle. Immunofluoresenssikokeiden ja kvantitatiivisen analysoinnin perusteella endosytoosi estyi, vaikkakin ero kontrollisoluihin oli ainoastaan 10 %. Lisäksi toinen immunofluoresenssikoe osoitti, että EV1:n infektiivisyys laski käytettäessä PLC-inhibiittoria. Immunofluoresenssikokeissa ongelmia aiheuttivat tyhjät ja rikkinäiset viruspartikkelit, jotka havaittiin EV1:n karakterisoinnin aikana läpäisyelektronimikroskoopilla. Leimautuneet tyhjät ja rikkinäiset partikkelit aiheuttivat todennäköisesti väärää signaalia immunofluoresenssikokeissa, joiden perusteella voitiin todeta, että viruksen puhdistaminen ja leimaaminen vaativat lisää optimointia. Suora kapsidileima voisi onnistuessaan toimia työkaluna tulevissa viruksen avautumiskokeissa ja livetutkimuksissa, jolloin vasta-aineleimauksiin liittyvä taustafluoresenssi saataisiin minimoitua. Lisäksi PLC-inhibiittori voisi mahdollistaa viruksen avautumisen tutkimisen solun pinnalla endosomaalisten rakenteiden sijaan.

Avainsanat: Echovirus 1, viruksen avautuminen, endosytoosin inhibiittori, fluoresenssileimaus

University of Jyväskylä **Abstract of Master´s Thesis**

Faculty of Mathematics and Science

Author: Mira Myllynen

Title of thesis: The Effect of PLC-Inhibitor on Echovirus 1 Internalization Probed with Fluorescently Labeled Echovirus 1

Finnish title: PLC-inhibiittorin vaikutus echovirus 1:n sisäänmenoon käyttäen fluoresoivasti leimattua echovirus 1:stä

Date: 14.8.2014 **Pages:** 42 + 4

Department: Department of Biological and Environmental Science

Chair: Cell and molecular Biology

Supervisor(s): Varpu Marjomäki , Artur Kazmertsuk

Abstract:

Echovirus 1 (EV1) belongs to the family of *Picornaviridae* and more specifically to the genus *Enterovirus*. EV1 is a small, non-enveloped RNA-virus which has a capsid consisting of four proteins VP1-VP4. EV1 has been shown to bind to $\alpha_2\beta_1$-integrin on the cell surface and then endocytosed inside the cell by a mechanism that resembles both caveolin-mediated endocytosis and macropinocytosis. Instead, uncoating and RNA release are poorly understood. Here, we have successfully purified EV1 with sucrose gradient and labeled the virus with an amine reactive dye. The results showed that for successful labeling, considerably low amount of dye is sufficient for signal detection, and according to end-point dilution assay, is necessary for maintaining virus infectivity. Capsid labeled EV1 was used in cellular studies where Phospholipase C-inhibitor (PLC-inhibitor) was tested as an endocytosis blocker. According to our hypothesis PLC-inhibitor blocks endocytosis, and as a result, virus remains on the cell surface. Indeed, based on immunofluorescence studies and quantification with Bioimage XD software, endocytosis was blocked, although difference to control cells was only 10%. Additionally, another immunofluorescence study showed that PLC-inhibitor decreased EV1 infection. Immunofluorescence studies were hindered by empty and disassembled virus particles, which were detected during EV1 characterization with transmission electron microcopy. Labeled empty and disassembled particles probably caused false signal in immunofluorescence studies, and thus, it was concluded that virus purification and labeling has to be more optimized for these kinds of studies. Fluorescent capsid label could provide us a tool for future uncoating and live imaging studies by minimizing non-specificity that is usually related to immunolabeling. In addition, PLC-inhibitor could enable uncoating studies to be carried out on the cell surface instead of endosomes.

Keywords: Echovirus 1, uncoating, endocytosis inhibitor, fluorescent labeling

Table of Contents

Abbreviations

A549 cells	Adenocarcinomic Human Alveolar Basal Epithelial cells
BSA	Bovine Serum Albumin
CAR	Coxsackievirus-Adenovirus Receptor
DAF	Decay-Accelerating Factor
DMEM	Dulbecco's Modified Eagle Medium
EV1	Echovirus 1
FBS	Fetal Bovine Serum
GMK cells	Green Monkey Kidney cells
HAVcr	Hepatitis A Virus cellular receptor
ICAM-1	Intercellular Adhesion Molecule 1
LDL-R	Low-Density Lipoprotein Receptor
MEM	Eagle's Minimum Essential Medium
PFA	Paraformaldehyde
PLC-inhibitor	Phospholipase C-inhibitor
PVR	Poliovirus Receptor
RGD motif	Arginine-Glycine-Aspartic acid motif
SAOS cells	Human Osteosarcoma cells
TEM	Transmission Electron Microscope

1 Introduction

1.1 Picornaviruses

Echovirus 1 (EV1) belongs to the family of *Picornaviridae* and more specifically to the genus *Enterovirus*. Picornaviruses are responsible of several diseases among humans and livestock. These for example include poliomyelitis, hepatitis A, foot- and –mouth disease and common cold. Some of the viruses are also thought to be related to chronic diseases such as diabetes 1 and asthma (Oberste and Pallansch, 2003; Kotaniemi-Syrjanen et al., 2003). Picornaviruses are small non-enveloped viruses which contain single stranded positive sense RNA as their genome. The genome of picornaviruses is encapsulated by an icosahedral capsid which consists of four different proteins VP1-VP4 where VP1-VP3 form the shell of the virus particle while VP4 is situated on the inner surface of the virion. The capsid is around 30 nm in diameter and is made up of 60 copies of each virus protein. The four different virus proteins form a protomer which are further assembled into pentameric subunits, 12 of which form the icosahedral capsid.

In general, the entry process and genome delivery of non-enveloped viruses is poorly understood. There are few members of picornavirus family, especially poliovirus and rhinoviruses, which have been actively studied to understand the early processes of infection. The general view of the infection steps has been obtained by studying different viruses, although at the same time, it has become clear that there are differences between picornavirus species.

1.2 Virus Interaction with its Receptor

During the early steps of infection viruses have to interact with receptors on the cell surface. In the family of picornaviruses, several different receptors have been identified

and receptor-virus interactions characterized. Picornavirus receptors include members that belong to the immunoglobulin superfamily, integrin family and low density lipoprotein receptor family (Table 1). In addition to the primary receptors, picornaviruses often need co-receptors for a productive infection (Shafren et al., 1997a; Shafren et al., 1997b; Shafren et al., 1997d).

1.2.1 EV1 Receptor

The receptor for EV1 is $\alpha_2\beta_1$-integrin, which mediates cell attachment to extracellular matrix via collagen and laminin (Bergelson et al., 1992; Bergelson et al., 1993). Integrins are transmembrane glycoproteins that transmit signals on both sides of plasma membrane by interacting with their extracellular ligands and activating signal pathways inside the cell (Hynes, 2002). Like many other integrins, $\alpha_2\beta_1$-integrin has an inserted domain of the integrin α-subunit (α_2I) to which ligand binds (Arnaout et al., 2005). The receptor can exist in different conformations and the inside-out signaling of $\alpha_2\beta_1$-integrin has been shown to be regulated by conformational activation and integrin clustering (Connors et al., 2007).

Binding site of both EV1 and collagen is the same, α_2I, but the mechanism of binding is different (King et al., 1995). Collagen binding to integrin is dependent on divalent cations whereas EV1 binding is not (Bergelson et al., 1993). In addition, unlike collagen which binds to an open conformation of integrin, EV1 binds to a closed conformation and inactive $\alpha_2\beta_1$-integrin (Jokinen et al., 2010). During its entry process EV1 also seems to rely on clustering of inactive integrin instead of any conformational changes of the receptor (Jokinen et al., 2010).

In many cases integrin ligands (i.e. some viruses) contain arginine-glycine-aspartic acid motif (RGD motif) which is a recognition site for integrin. However, ligand binding to EV1 receptor α2β1-integrin is RGD independent (Pierschbacher and Ruoslahti, 1984). Enteroviruses and major group human rhinoviruses have a depression around the fivefold axis symmetry, the canyon, in which receptors bind, and instead of binding to a RGD motif, also the interaction of EV1 and its receptor is via the canyon (Xing et al., 2004).

Even though the main receptor for EV1 is $\alpha_2\beta_1$-integrin, also β_2 microglobulin is needed for the entry of the virus. It is still unknown how β_2 microglobulin exactly affects EV1 entry, but it has been shown that the entry is inhibited by antibodies against β_2 microglobulin (Marjomaki et al., 2002; Ward et al., 1998).

Table 1. Identified picornavirus receptors. Modified from Michael G. Rossmann, Yongning He and Richard J. Kuhn review article Picornavirus–receptor interactions 2002, table2.

Virus	Receptor	Reference
Major-group human rhino virus (90 serotypes)	ICAM-1	(Greve et al., 1989)
Minor-group human rhino virus (10 serotypes)	LDL-R	(Hofer et al., 1994)
Poliovirus (3 serotypes)	PVR	(Mendelsohn et al., 1989)
Coxsackie virus B (6 serotypes)	CAR, DAF	(Mendelsohn et al., 1989; Bergelson et al., 1997)
Coxsackie virus A 21	ICAM-1	(Shafren et al., 1997c)
Coxsackie virus A 9	$\alpha_v\beta_3$-integrin	(Berinstein et al., 1995)
Echovirus (10+serotypes)	DAF	(Mendelsohn et al., 1989)
Echovirus (serotypes 1 and 8)	$\alpha_2\beta_1$-integrin	(Bergelson et al., 1992)
Hepatitis A virus	HAVcr-1	(Kaplan et al., 1996)
Foot and mouth disease virus (7 serotypes)	αvβ3 and αvβ6 integrin, heparan sulfate	(Berinstein et al., 1995; Jackson et al., 2000; Jackson et al., 1996)
Theiler's murine virus	Sialic acid	(Zhou et al., 2000)

1.3 Internalization of Picornaviruses

After binding to their receptors, picornaviruses are endocytosed. It was earlier suggested that poliovirus can also enter the cell directly through plasma membrane, but more recent studies show that poliovirus is endocytosed (Brandenburg et al., 2007). In addition to different receptors, picornaviruses also use different kinds of entry routes during infection and the receptor largely determines the entry pathway. However, the connection between receptor and entry route is not unambiguous and viruses may enter different pathways even if they use the same receptor (Brandenburg et al., 2007; Coyne and Bergelson, 2006). In

addition, many picornaviruses can also adapt to different entry routes and expand their tropism (Martinez et al., 1997; Hughes et al., 1995; Reischl et al., 2001).

Despite the diversities in viral entry pathways, several endocytic routes for picornaviruses have been identified, often by using markers for different routes and inhibiting entry pathways. One of the best known entry pathways is clathrin-mediated endocytosis, where the cargo (i.e virus) is first centralized to a clathrin-coated pit on the plasma membrane, after which a clathrin-coated vesicle forms and the cargo is internalized. The vesicles are then uncoated and delivered to early endosomes. Clatrin-mediated endocytosis has been suggested to be an entry route for at least foot and mouth disease virus, some minor and major group human rhinoviruses (see review: (Fuchs and Blaas, 2012) and Hepatitis A virus (Bishop, 1998). Many viruses that use clathrin-mediated entry route need to encounter low pH to complete their entry (Berryman et al., 2005; Bayer et al., 1998; Grunert et al., 1997). Other endocytic route identified for picornaviruses is caveolin mediated endocytosis, which has been shown to be an entry pathway for some echoviruses and coxsacie viruses. Poliovirus, on the other hand, uses a route independent of clathrin, caveolin and flotillin and the pathway has been shown to be actin dependent (Brandenburg et al., 2007) It has been shown that also major group human rhinovirus 14 does not depend on clathrin, caveolin and flotillin while infecting Rhabdomyosarcoma cells expressing ICAM-1(Khan et al., 2010). In these cells, entry route of human rhinovirus 14 seems to have some characteristics of macropinocytosis, which is characterized as non-selective, actin-driven internalization of solute molecules.

1.3.1 Entry Pathway of EV1

On the contrary to many other picornaviruses, enteroviruses (except minor group rhinoviruses) are stable in acidic pH, and do not rely on the decrease in pH during their entry. In addition, the entry route for some echoviruses and coxsackie viruses is not clathrin-dependent, but instead, is caveolin-mediated.

Earlier studies suggested that, after EV1 binds to its receptor $\alpha_2\beta_1$-integrin on the cell surface, both EV1 and receptor are internalized by caveolae-mediated endocytosis

(Marjomaki et al., 2002). Caveolae are special type of lipid rafts related to cholesterol trafficking, cellular signaling and transport (Quest et al., 2004). Characteristically caveloae are small invaginations on the plasma membrane and contain caveolin-1 as their main protein (Parton, 1996). Internalization of caveolar vesicles can be triggered by ligand binding to its receptor, after which caveolar vesicles accumulate in caveosomes which are caveolin-1 containing structures inside the cell (Pelkmans et al., 2001). It has been previously shown that after receptor binding, EV1 is rapidly internalized into caveosomes by a mechanism that is dependent on dynamin II, cholesterol and signaling events (Pietiainen et al., 2004) and in addition, that the internalization is not dependent on actin or microtubules.

More recently it has been shown that the majority of EV1 does not accumulate in caveolin-1 positive structures immediately, but instead, the early entry pathway resembles macropinocytosis (Karjalainen et al., 2008). This has been shown by using inhibitors related to fluid-phase endocytosis and macropinocytosis, which also seem to block the internalization of EV1 and $\alpha_2\beta_1$-integrin (Karjalainen et al., 2008). Instead of internalization through caveolae, EV1 entry originates from lipid rafts, where the virus induces clustering of $\alpha_2\beta_1$-integrin and both receptor and virus are internalized into tubulovesicular structures. These structures mature further into larger multivesicular bodies (Karjalainen et al., 2008). This pathway is still related to caveosomes, and it has been suggested that multivesicular bodies are able to fuse with earlier internalized caveosomal structures that contain caveolin-1, and may then be considered as late caveosomes (Karjalainen et al., 2008). In addition to EV1, Coxsackie virus A9 has been recently shown to be dependent on non-acidic multivesicualar bodies during infection (Huttunen et al., 2014).

1.4 Virus Uncoating

Picornaviruses have to be stable enough to withstand different conditions inside their host, but still, they have to be able to release their genome inside the host during infection. Once inside the cell, the virion is still inside a cellular vesicle and has to cross a membrane and

free its genome so that RNA replication can begin. Thus, viral particles have to be metastable that can undergo structural transformations, which allow membrane cross and genome release.

It has been observed that poliovirus and some other enteroviruses and rhinoviruses change their conformation after binding to their receptors. When the virus binds to its receptor, the conformation of virus capsid changes and the virus particle becomes a so-called 135S-particle, which has a different sedimentation rate in sucrose gradient than a native virus (160S) (Fricks and Hogle, 1990). As the infection proceeds, particles change further to 80S particles where RNA has been released (Fricks and Hogle, 1990). These structural changes of virus particle during early steps of infection have also been observed with EV1 even though the receptor has not been shown to induce the structural changes directly (Marjomaki et al., 2002).

It is known for poliovirus, that in the 135S particle, both VP4 and the N-terminus of VP1 are externalized (Fricks and Hogle, 1990) and that the 80S particle additionally lacks RNA (Belnap et al., 2000). Other differences between 135S and native particles are different antigenicity and sensitivity to proteases (Fricks and Hogle, 1990). In addition, unlike native particles which are hydrophilic, 135S particles are hydrophobic and are able to bind membranes in the form of liposomes via the externalized amino terminus of VP1 (Fricks and Hogle, 1990). In addition to membrane bound receptors, 135S particles can also be formed with solubilized receptors (Kaplan et al., 1990) or by heating viruses over physiological temperatures (50 °C) in low ionic-strength buffer (Curry et al., 1996).

1.4.1 RNA Release

The uncoating process and RNA release of enteroviruses is still poorly understood and the mechanism by which VP4, the amino terminus of VP1 and RNA are released from the virus capsid is still unknown. It has been shown with poliovirus that 135S and 80S particles are 4% bigger than native particles and do not have exit sites for VP4, amino terminus of VP1 and RNA (Belnap et al., 2000). Previous studies suggested that VP4, N-terminus of VP1 and RNA are released from the particle through a fivefold axis channel

(Hadfield et al., 1997; Rossmann et al., 2000) . It was also suggested in the old model that five copies of externalized VP1 and VP4 would form a pore by interacting with the membrane near the 5-fold axis, thus providing a channel where RNA can be released (see review: Rossmann et al., 2000). However, it was showed later with the reconstruction of poliovirus 135S particle that there is not enough space for five copies of VP1 N-terminus in the fivefold mesa (Belnap et al., 2000). In addition, it has been shown for poliovirus that VP1 exits from the base of the canyon instead of associating with the fivefold mesa (Levy et al., 2010).

In contrary to previous studies, it has been more recently suggested with the help of cryo-electron microscopy that in polioviruses, RNA is released from the capsid near the 2-fold axis at the base of the canyon, instead of 5-fold axis (Bostina et al., 2011). Even more recent studies with Enterovirus 71 and Coxsackievirus A16 also support the idea that the exit site for RNA and internal capsid proteins is near 2-fold axis (Lyu et al., 2014; Ren et al., 2013). RNA is additionally thought to exit the virion from a single site to avoid entanglement with the capsid (Bostina et al., 2011). However, it is still unknown how this single site is selected out of 60 equivalent sites or how viruses can find the exit site that is towards the membrane.

In addition, the cryo-electron microscopy studies suggest that RNA must be unwound while it exits the capsid (Bostina et al., 2011). Also previous studies with light microscopy indicate that RNA is folded inside the virion but is released as a single stranded RNA (Brandenburg et al., 2007). It was also showed with live light microscopy studies that once poliovirus is internalized by endocytosis, RNA is released fast and efficiently into the cytoplasm (Brandenburg et al., 2007). Efficient and rapid RNA release could further suggest that a continuous channel is formed which enables translocation of RNA from virion, through the membrane and into the cytoplasm (Brandenburg et al., 2007). The most recent studies with rhinoviruses have also shown that, in addition to be single stranded, RNA has to have certain direction, as the release starts from the 3’-end (Harutyunyan et al., 2013). Fixed direction could further suggest that, when the virus particle is assembled, the 3’-end is located near the capsid wall, close to the place of RNA release (Harutyunyan et al., 2013).

2 Aim of the Study

The main focus of this thesis was in the early events of EV1 infection and the aim was to lay foundation for future uncoating studies by optimizing fluorescent capsid labeling of EV1. First, EV1 was purified with sucrose gradient, after which the purity and infectivity of the virus was characterized with different methods. Second, the purified EV1 was labeled fluorescently with an amine reactive dye, after which characterization was also carried out to find out optimal conditions for labeling.

Fluorescently labeled EV1 was used in cellular experiments where the aim was to block endocytosis of the virus with Phospholipase C inhibitor (PLC-inhibitor), and as a result, leave the virus on the cell surface. Internalization of EV1 was evaluated and quantified with confocal microscopy and Bioimage XD-software. The functionality of PLC-inhibitor was additionally confirmed by studying EV1 infection in the presence of the inhibitor. The purpose was to create a system, where EV1 uncoating could be studied on the cell surface, which would enable mimicking of endosomal environment in the future uncoating studies.

3 Materials and Methods

3.1 Virus Purification

Green Monkey Kidney (GMK) cells were cultured in 80 cm^2 flasks in Eagle's Minimum Essential Medium (MEM, Gibco Life Technologies, South America) supplemented with 10% Fetal Bovine Serum (FBS, Gibco Life Technologies, United Kingdom), 1% L-Glutamine and 1% penicillin and streptomycin antibiotics. In order to get sufficient cell mass, GMK cells were next grown in 175 cm^2 flasks, where infection was carried out for sub-confluent cells. Infection was carried out in MEM with 1% FBS without antibiotics. EV1 was added and infection was allowed to proceed for one day at + 37 °C under 5 % CO_2.

Three freeze-thaw cycles were carried out to previously EV1 infected GMK cells. Cells were pelleted by centrifuging at 6080 rpm for 45 min at + 4 °C in Avanti centrifuge with JLA 10.500 rotor. After centrifugation, 7% (w/v) PEG and 2.2% (w/v) NaCl were added to virus supernatant and stirred overnight at + 4 °C.

Virus was pelleted by centrifuging at 8000 rpm for 45 min at + 4 °C in Avanti centrifuge with JLA 10.500 rotor. Pellet was scraped with 3 ml of R-buffer (10 mM Tris-HCL, pH 7.5; 0.2 M NaCl; 50 mM $MgCl_2$ and 10% glycerol) after which sodium deoxycholate (3 mg ml^{-1}) and 100% NP-40 (6 µl ml^{-1}) were added. Mix was incubated on ice for 30 min and after incubating, virus was centrifuged at 2500 rpm for 15 min at + 4 °C in Hermle centrifuge Z 513K. Supernatant was added on top of a linear 10%-40% sucrose gradient and centrifuged at 30000 rpm for 3 h at + 4 °C in Beckman ultracentrifuge with SW41 T1 rotor. After centrifuging, 500 µl fractions were collected from the top and OD_{260} was measured with Nanodrop spectrophotometer 1000 (Thermo Scientific) to identify virus containing fractions.

Virus containing fractions were dialyzed with Spectra/ Por® Micro FLOAT-A-LYZER® with Biotech cellulose ester membranes (Spectrum Laboratories Inc., USA). The dialysis

column with 50 kD MWCO was prepared according to instructions by the manufacturer, after which virus sample was dialyzed against 2 mM $MgCl_2$/PBS buffer. Buffer was changed after two and four hours after which the sample was dialyzed overnight.

Sample was collected from the dialysis column and the column was rinsed with 10 ml of 2 mM $MgCl_2$/PBS buffer which was also collected. In total 20 ml of sample was then concentrated in Beckman ultracentrifuge with 45 Ti rotor. Centrifugation was carried out at 35000 rpm for 2 h at + 4 °C after which virus pellet was dissolved in 100 µl of 2 mM $MgCl_2$/PBS buffer and the virus concentration was determined with Nanodrop spectrophotometer 1000 (Thermo Scientific). In total three batches EV1#1, #2, and #3 were purified.

3.2 Fluorescent Labeling of EV1 with AlexaFluor594 and AlexaFluor488

For optimal fluorescent labeling of the capsid, the pH of EV1 was first adjusted to 8.3 or 9.0 with 1 M sodium bicarbonate buffer. EV1 was then labeled with an amine reactive dye Alexa fluor®594 or Alexa fluor®488 (Invitrogen, Molecular Probes, USA) containing a succinimidyl ester linker (10 mg ml^{-1} in dimethylsulphoxide). Three different dye-to-protein ratios were tested: 37:1, 10:1, and 5:1 and the virus was incubated with the dye for 1 h, at room temperature and in the dark. During the incubation, virus / dye mix was tapped and centrifuged few times.

First, the virus amount in moles was calculated (Eq.3.1).

$$n_{EV1} = \frac{c_{EV1} \times V_{EV1}}{MW_{EV1}} \tag{3.1}$$

Where c_{EV1} is the concentration of the virus based on measurements with Nanodrop spectrophotometer 1000 (Thermo Scientific) and Lambert Beer's equation, V_{EV1} is the sample volume and MW_{EV1} is the molecular weight of EV1.

Next, the amount of dye in moles was calculated based on virus amount in moles and the desired dye-to-protein ratio, e.g. 37:1 (Eq.3.2).

$$\frac{n_{label}}{n_{EV1}} = 37 \tag{3.2}$$

Where n_{label} is the amount of dye in moles and n_{EV1} is the amount of virus in moles.

Finally, the volume of the dye needed for labeling was calculated (Eq.3.3).

$$V = \frac{n_{label} \times MW_{label}}{c_{label}} \tag{3.3}$$

Where n_{label} is the amount of dye in moles, MW_{label} is the molecular weight of the dye and c_{label} is the concentration of the dye. Values used in the calculations are presented in table 2.

3.3 Column Purification of Labeled EV1

After 1 h incubation with the dye, labeled EV1#1 was purified with a gravity flow column (Illustra NAP-5 column, GE healthcare, United Kingdom) to remove the excess dye. First 1 ml of 2 mM $MgCl_2$/PBS buffer was let to flow through the column after which 50 µl of sample was loaded. Then, 450 µl of the same buffer was added and let flow through, after which 100 µl of buffer was added ten times and fractions were collected into separate tubes. OD_{260} was measured for every fraction with Nanodrop spectrophotometer 1000 (Thermo Scientific). Nanodrop results showed an extra peak around 280 nm in the absorption spectrum and thus virus fractions were further purified with dialysis. Column purification was carried out for only EV1#1 and omitted when EV1#2 and EV1#3 were labeled. Excess dye was removed from EV1#2 and #3 only by dialyzing.

3.4 Dialysis of Fluorescently Labeled EV1

The excess dye was removed by dialysis carried out with Spectra/ Por® Micro FLOAT-A-LYZER® with Biotech cellulose ester membranes (Spectrum Laboratories Inc., USA). The dialysis casette with 50 kD MWCO was prepared according to instructions by the manufacturer after which fluorescently labeled virus was dialyzed against 2 mM $MgCl_2$/PBS buffer. Buffer was changed after two and four hours after which the sample was dialyzed overnight.

3.5 Calculation of the Degree of Labeling

Based on Nanodrop spectrophotometer 1000 (Thermo Scientific) results, concentration of the labeled virus was calculated (Eq.3.4).

$$A_{protein} = A_{260} - A_{max} \times CF_{260} \quad (3.4)$$

Where A_{260} is the total absorption at 260 nm, A_{max} is the absorption at the absorbance maximum of the dye and CF_{260} is A_{260} for free dye / A_{max} for free dye.

The concentration of the virus protein was determined with Lambert Beer's equation using values presented in table 2. The obtained EV1 concentration was multiplied by 0.7 to obtain the concentration of the viral proteins which comprise around 70% of the virion.

Additionally, the degree of labeling (DOL) was calculated (Eq.3.5).

$$DOL = \frac{A_{max} \times MW_{EV1}}{[EV1] \times \varepsilon_{dye}} \quad (3.5)$$

Where A_{max} is the absorption at the absorbance maximum of the dye, MW_{EV1} is the molecular weight of EV1, *[EV1]* is the protein concentration in mg ml^{-1} and ε_{dye} is the extinction coefficient of the dye at its absorbance maximum.

Finally, the amount of fluorophores per virus particle was obtained (Eq.3.6).

$$Fluorophores\ per\ virus\ particle = DOL\ \times 4\ \times 60 \tag{3.6}$$

Values used in the calculations are presented in Table 2.

Table 2. Values used in the calculations.

Variable	Value
Molecular weight of EV1 (MW_{EV1})	23500 g mol^{-1}
Extinction coefficient of EV1	7.7
Molecular weight of the dye (MW_{label}), Alexa594	819.85 g mol^{-1}
Molecular weight of the dye (MW_{label}), Alexa488	643.41 g mol^{-1}
Extinction coefficient of the dye at its absorbance maximum (ε_{dye}), Alexa594	73000 $cm^{-1}M^{-1}$
Extinction coefficient of the dye at its absorbance maximum (ε_{dye}), Alexa488	71000 $cm^{-1}M^{-1}$
A_{260} free dye/ A_{max} free dye (CF_{260}), Alexa594	0.4
A_{260} free dye/ A_{max} free dye (CF_{260}), Alexa488	0.3

3.6 Determination of Virus Infectivity with End-point Dilution

Infectivity of EV1 was determined with end-point dilution assay, where GMK cells were cultured in 96-well plates for one day in MEM supplemented with 10% FBS, 1% Glutamax and 1% penicillin/streptomycin antibiotics. Infection was carried out by preparing a dilution series in MEM supplemented with 1% FBS and 1% Glutamax and infection was followed daily. After three days of infection, cells were dyed with crystal violet (3.4 g l^{-1} crystal violet; 5 g l^{-1} $CaCl_2$; 10% ethanol; 18.5 % formaline and 35mM Tris-Base) for 10 min. Infected cells detach from the plate and will be washed, so consequently, only live and dyed cells will remain on the plate. Based on eight replicates, the infectivity was determined by calculating the number of dyed and non-dyed wells.

3.7 Characterization of EV1 with SDS-Polyacrylamide Gel Electrophoresis

Purity of unlabeled virus and fluorescently labeled viruses were investigated with 12% SDS- polyacrylamide gel electrophoresis (PAGE). Loading buffer (5x concentrated) containing β-mercaptoethanol was added to samples containing 2.5-5 µg of protein, and also a pre-stained protein ladder Page ruler ^{TM} plus (Thermo Scientific, Lithuania) was loaded. The gel was stained with Coomassie blue (R250, BioRad) to detect the virus proteins, after which the gel was exposed with UV-light, to detect the fluorescently labeled virus proteins (BioRad).

3.8 Characterization of EV1 with Transmission Electron Microscope (TEM)

Butwar-coated copper grids (prepared in Biocenter Oulu) were first made hydrophilic by glow discharging with EMS/SC7620 Mini sputter coater according to the instructions by the manufacturer. Virus sample was added on the grid and incubated for 15 seconds after which the excess virus was blotted with Whatman 3 mm paper. Then, viruses were negatively stained by adding 1% phosphotungstic acid (in water, pH 7.0) on the grid for one minute after which the excess stain was blotted with Whatman 3 mm paper. Samples were dried overnight and imaged with JEM-1400 transmission electron microscope.

3.9 Fluorescence Detection of Labeled EV1 with Fluorescence Microscope

Labeled viruses were imaged with Zeiss fluorescence microscope (Carl Zeiss, Axio Observer) to verify that the fluorescence was detectable. Imaging was done with 63 x objective (NA 1.3) and signal was collected through appropriate filter setting provided by

the microscope (470 and 590). Imaging was done with Axiocam MR using 500-7000 ms integration time without averaging.

3.10 Immunofluoresence and Confocal Microscopy

Two cell lines were used in immunolabeling experiments: Human osteosarcoma cells (SAOS) stably transfected with $\alpha_2\beta_1$-integrin (Marjomaki et al., 2002) and adenocarcinomic human alveolar basal epithelial cell line, A549 cells. Cells were cultivated on tissue plates with coverslips on the bottom. The cell plates were prepared one or two days before the experiment and cells were cultured in Dulbecco's Modified Eagle Medium (DMEM, Gibco Life Technologies, United Kingdom) supplemented with 10% FBS (Gibco, Life Technologies), 1% Glutamine and 1% penicillin/streptomycin antibiotics. The immunolabelings were carried out with antibodies and antibody dilutions presented in table 3. Mounting was carried out with Prolong® gold antifade reagent supplemented with DAPI (Molecular Probes, Life Technologies, USA). Immunolabeled samples were imaged with Olympus microscope IX81 with FluoView-1000 confocal setup.

Table 3. Antibodies and their final concentrations used in the experiments.

Primary/secondary	Antibody	Final concentration	Origin
Primary	rabbit anti-EV1	1:150 from affinity purified serum	(Marjomaki et al., 2002)
Primary	anti-integrin a211e10	4 µg ml^{-1}	from Fedor Berditchevski, Institute of Cancer Studies, Birmingham, United Kingdom
Primary	anti-integrin MCA2025	6.7 µg ml^{-1}	Serotec Inc.
Secondary	Goat anti-mouse AlexaFluor488	5 µg ml^{-1}	Molecular Probes, Invitrogen/ USA
Secondary	Goat anti-rabbit AlexaFluor555	5 µg ml^{-1}	Molecular Probes, Invitrogen/ USA

3.10.1 Colocalization of Alexa594 Labeled EV1 with $\alpha_2\beta_1$-Integrin

The experiment was carried out with two different cell lines: SAOS and A549. Also two different anti-integrin antibodies were tested: a211E10 and MCA2025. Samples included non-labeled EV1 and Alexa594 labeled EV1 (dye/protein 37:1, pH 9.0) with each anti-integrin antibody. EV1 that was not fluorescently labeled was labeled with antibodies.

Cell plates with coverslips were prepared one day before with 1:3 surface dilution of SAOS and 1:5 surface dilution of A549 cells from confluent cultures. EV1, that was not fluorescently labeled, was diluted 1:1000 (infectivity 10^{12} pfu ml^{-1}) and Alexa594 labeled EV1 1:250 because of the lower infectivity (infectivity 10^{8} pfu ml^{-1}). Viruses were diluted in DMEM supplemented with 1% FBS (Gibco, Life Technologies) and 1% Glutamine and bound on cells by incubating for 1 h on ice, after which the excess virus was washed with PBS containing 0.5% bovine serum albumin (BSA). Cells were fixed with 4% paraformaldehyde (PFA) for 30 min on ice and after fixation, cells were washed with PBS. Primary antibodies rabbit anti-EV1 and a211e10 or MCA2025 were added on cells, and cells were incubated for 1 h on ice. Primary antibodies were diluted in 3 % BSA/PBS and final concentrations were as in table 3.

After incubation on ice, cells were extensively washed with PBS, after which secondary antibodies were added. Secondary antibodies goat anti-mouse AlexaFluor488 and goat anti-rabbit AlexaFluor555 were also diluted to 3% BSA/PBS and final concentrations were as in table 3. After 30 min incubation on ice in the dark, cells were extensively washed with PBS and mounted.

3.10.2 Inhibition of EV1 Internalization with U73122

The experiment was carried out with two different cell lines: SAOS and A549. Plates with coverslips were prepared two days before with 1:3 surface dilutions from confluent cultures. Cells were treated with Phospholipase C-inhibitor (PLC-inhibitor) U73122 and infected with Alexa488 labeled virus. After 2 h, cells were fixed and immunolabeled. The

concentration of U73122 was 10 µM, diluted in DMEM supplemented with 1% FBS (Gibco, Life Technologies) and 1% Glutamine. Cells were first pretreated with U73122 for 30 min at + 37 °C and then washed. As a control, cells were not treated with U73122 but infected with Alexa488 labeled EV1, and after that, fixed and labeled 0 h and 2 h post infection (p.i.). Also negative controls without virus were included to remove the background signal during imaging.

Alexa488 labeled EV1 (infectivity 10^9 pfu ml^{-1}) diluted 1:250 in DMEM supplemented with 1% FBS (Gibco, Life Technologies) and 1% Glutamine was bound on cells on ice for 1 h, after which excess virus was washed with 0.5% BSA/PBS. After binding the virus, cells were either fixed or incubated in DMEM supplemented with 10% FBS (Gibco, Life Technologies), 1% Glutamine and 1% penicillin/streptomycin antibiotics at + 37 °C for 2 h. Cells were fixed with 3% PFA for 15 min on ice, after which they were washed with 50 mM ammonium chloride. Primary antibody anti-EV1 (Table 3) was next added on cells on ice for 45 min, after which cells were extensively washed with PBS. Secondary antibody goat anti-rabbit conjugated with AlexaFluor555 (Table 3) was added on cells on ice for 30 min and after that cells were washed extensively with PBS. Finally, cells were mounted.

3.10.3 EV1 Infection in U73122 Treated Cells

The experiment was carried out with two different cell lines: SAOS and A549. Plates with coverslips were prepared two days before with 1:3 surface dilutions from confluent cultures. Cells were treated with 10 µM U73122 for 30 min before the experiment and infected with Alexa488 labeled virus. As a control, cells were infected with Alexa488 labeled virus without U73122 treatment, and also negative control without virus was included to remove the background signal during imaging.

Alexa488 labeled EV1 (infectivity 10^9 pfu ml^{-1}) was diluted 1:250 in DMEM supplemented with 1% FBS (Gibco, Life Technologies) and 1% Glutamine and bound on cells on ice for 1 h. Excess virus was washed with 0.5% BSA/PBS and cells were incubated in DMEM supplemented with 10% FBS (Gibco, Life Technologies), 1% Glutamine and 1% penicillin/streptomycin antibiotics at + 37 °C for 6 h.

Cells were fixed with 4% PFA for 30 min at RT after which they were washed and left in the fridge in PBS. Samples were immunolabeled the next day. Cells were first permeabilized with 0.2% Triton X-100 for 5 min. Primary antibody anti-EV1 (Table 3) was next added on cells and incubated at RT for 45 min, after which cells were washed extensively with PBS. Secondary antibody goat anti-rabbit conjugated with AlexaFluor555 (Table 3) was added on cells at RT for 30 min. Finally, cells were extensively washed with PBS and mounted.

3.11 Data Analysis of the Microscopic Data

Quantification of colocalization was carried out with BioImage XD software (Kankaanpaa et al., 2012). Ten cells from three different experiments were imaged with confocal microscope and the colocalization was then quantified with BioImage XD. The colocalization thresholds were set manually so that background fluorescence was eliminated. Analysis was carried out by calculating the percentage of Ch1 or Ch2 voxels colocalizing with Ch2 or Ch1 voxels. In the study of EV1 colocalization with $\alpha_2\beta_1$-integrin, EV1 channel (Ch2) was compared to integrin channel (Ch1) to see how EV1 colocalizes with integrin which is found in abundance on the cell surface. In the U73122 study, Alexa488 labeled EV1 (Ch1) was compared to antibody labeled EV1 (Ch2).

In the infection study with U73122, 600-800 cells per each sample were checked for infection. First, nuclei were calculated with segmentation tool of Bioimage XD, and after that, infected cells were counted by hand. The number of infected cells was then compared to total number of cells and infection percentage was obtained.

3.12 Statistical Testing

Statistical comparison between samples was carried out by applying a t-test. Because the data contained percentages, the t-test was applied after transforming the binominal distribution of the data to follow normal distribution with arcsin$\sqrt{}$.

4 Results

4.1 EV1 Purification and Characterization

The first aim of the study was to produce pure EV1. In total, three batches EV1#1, #2, and #3 were purified and characterized. Purification was carried out using 10-40% sucrose gradient where virus particles were separated from cellular material according to mass. Virus was collected from the gradient according to OD_{260} measurements that were carried out for every 500 µl fraction with Nanodrop spectrophotometer (Figure 1A). According to the OD_{260} measurements, three fractions were collected for dialysis, the main fraction with the highest OD_{260} value and one fraction from both sides of the main fraction. Clear virus peak was detected in every batch but the virus was in different fraction in the gradient every time (Figure 1A).

After purification, the virus was run on 12% SDS-PAGE gel to verify that cellular proteins were eliminated and sample contains viral proteins VP1-VP3 which are between 35-25 kDa in size and VP4 which is 7 kDa in size. Every purified EV1 batch contained viral proteins, and bands were detected between 35-25 kDa, but VP4 could not be observed. EV1#1 and #2 were pure according to SDS-PAGE while EV1#3 contained some impurities (Figure 1B). Virus was also imaged with transmission electron microscope (TEM) after negative staining to see that virus particles were intact (Figure 1C). Intact particles are observed as white spots surrounded by negative stain, while empty particles have dark interior, since the capsid is penetrated by the stain. Intact particles were observed in every batch, and only some empty and disassembled particles in batches #1 and #2. However, EV1#3 contained more also empty and disassembled particles (Figure 1C).

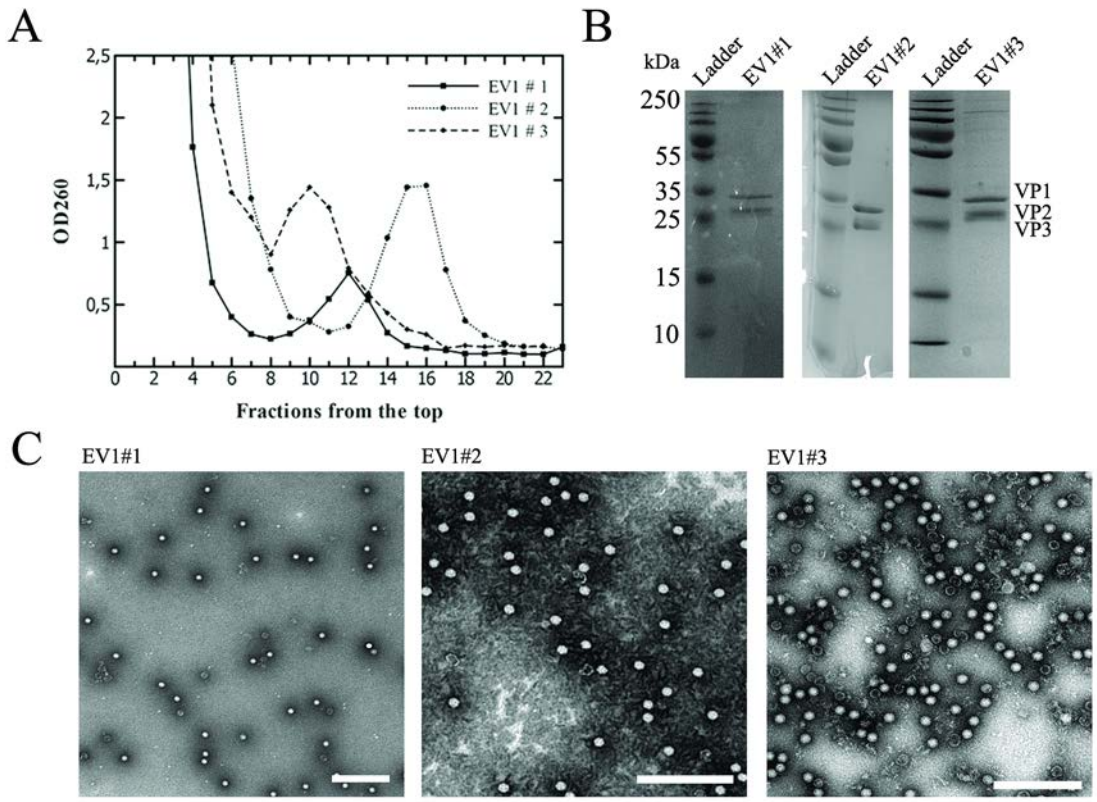

Figure 1. Purification of EV1#1, #2 and #3 was carried out using a linear 10-40% sucrose gradient. (A) OD_{260} was measured for fractions collected from the gradient. (B) EV1 was run on 12% SDS-PAGE gel to verify the purity of the virus. The size of VP1-VP3 proteins is between 32-26 kDa and they can be detected from the gel. VP4 (size 7 kDa) is not visible. Also Protein Ladder Page Ruler was included. (C) EV1 particles were negatively stained and imaged with TEM. A large amount of particles are intact but additionally disassembled and empty particles are detected. Scale bars 500 nm.

4.2 Fluorescent Labeling of EV1 and Characterization of Labeled Virus

After purification, the capsid of EV1 was fluorescently labeled with an amine reactive dye which contained succinimidyl ester linker. The target for amine modification is usually primary amines of lysine residues and the reaction is highly pH dependent. The pH of EV1 was first set to 8.3 or 9.0 to protonate lysine residues, and EV1 was then incubated with previously calculated amount of dye for 1 h at RT, after which excess dye was removed by dialysis. Three different virus batches were produced EV1#1, #2, and #3 and also three different dye-to-protein ratios were tested: 37:1, 10:1, and 5:1 respectively. Additionally,

two different labels were tested, AlexaFluor594 for first two batches and AlexaFluor488 for the third batch (from now on referred to as $EV1_{L594}$ and $EV1_{L488}$ respectively).

The degree of labeling was calculated according to Nanodrop spectrophotometer measurements (for more details see materials and methods) (Table 4). There are 23 lysine residues in VP1-VP4 proteins in total, but because not all lysine residues are on the surface, the theoretical degree of labeling is under 1380. Based on our results, the degree of labeling was under 1380 for each labeling, as expected. However, the degree of labeling increased as the dye-to-protein ratio was decreased (Table 4.).

Table 4. The amount of dye used for EV1 labeling and the corresponding degrees of labeling.

EV1 batch	Dye-to-protein ratio	Degree of labeling (fluorophores/particle)
$EV1_{L594}$ # 1 pH 8.3	37:1	135
$EV1_{L594}$ # 1 pH 9.0	37:1	124
$EV1_{L594}$ # 2 pH 8.3	10:1	140
$EV1_{L594}$ # 3 pH 8.3	5:1	542
$EV1_{L488}$ # 3 pH 8.3	5:1	307

After labeling, virus was characterized with 12% SDS-PAGE. SDS-PAGE gel bands were first exposed with UV-light to detect the fluorescently labeled viral proteins, and after that, the gel was stained with Coomassie Blue to detect the virus proteins (Figure 2A). The fluorescence of capsid labeled EV1 was additionally detected with fluorescence microscope (Figure 2B). Virus particles were imaged with TEM to evaluate whether the virus was still intact after pH change and labeling (Figure 2C).

Two different pH (8.3 and 9.0) were tested in the first labeling where dye to protein ratio was 37:1. Based on SDS-PAGE results, both batches were pure and contained labeled virus proteins (Figure 2A). In addition, the fluorescence of labeled virus (pH 9.0) was detectable according to fluorescence microscopy results (Figure 2B). The intactness was additionally checked with TEM, and based on the results, virus particles were still intact after pH change and labeling (Figure 2C). However, pH 9.0 was also observed to break down virus particles, which was judged by detection of pentameric sturctures (Figure 2C, red circle).

Since it was noticed that pH 8.3 was sufficient for labeling and that pH 9.0 broke down more particles, the following labelings, where dye-to-protein ratio was 10:1 and 5:1, were carried out in pH 8.3. Viral proteins were observed on SDS-PAGE gel and the fluorescence was detectable with fluorescence microscope, both when 10:1 and 5:1 dye-to-protein ratio was used (Figure 2A and 2B). Additionally, the particles were still intact according to TEM results (Figure 2C

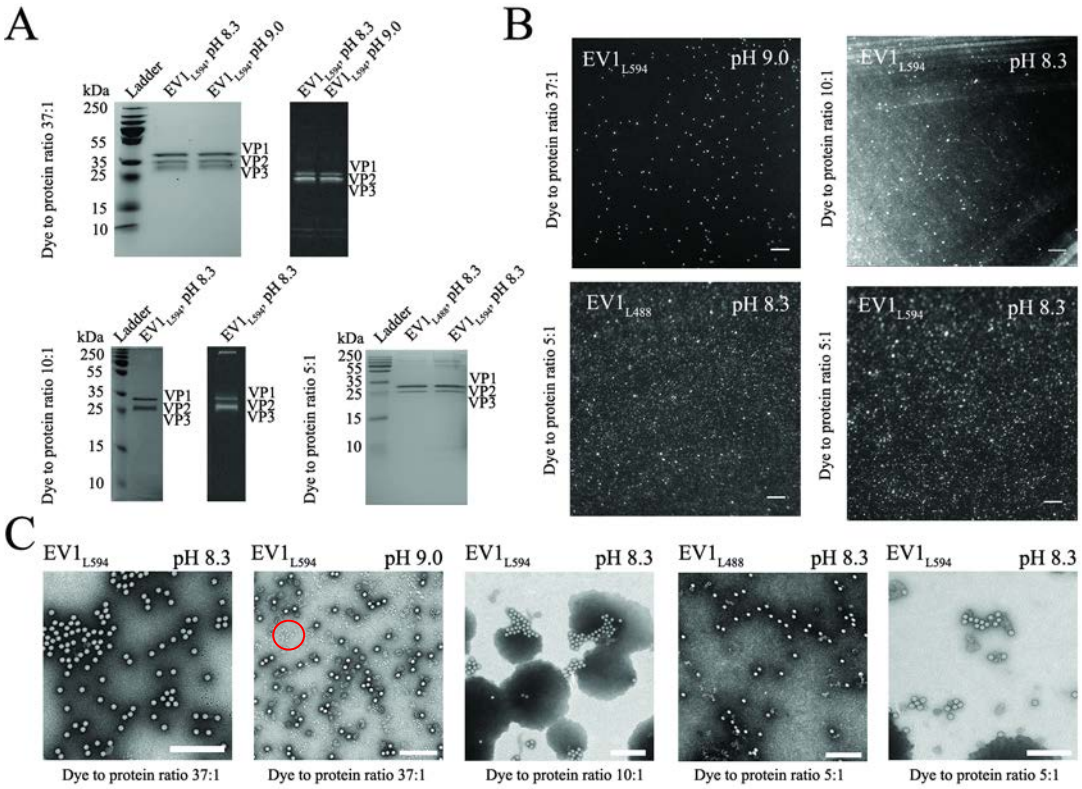

Figure 2. Labeling of EV1 with an amine reactive dye Alexa594 ($EV1_{L594}$) or Alexa488 ($EV1_{L488}$). Three dye-to-protein ratios were tested: 37:1, 10:1, and 5:1. (A) 12% SDS-PAGE gel where viral proteins were stained with Coomassie blue to detect the viral proteins. The size of VP1-VP3 proteins is between 32-26 kDa and they can be detected from the gel. VP4 (size 7 kDa) is not visible. SDS-PAGE gel was also exposed with UV-light to detect labeled virus proteins. (B) The fluorescence of $EV1_{L594}$ and $EV1_{L488}$ was also detected with fluorescence microscope. Scale bars 10 µm. (C) $EV1_{L594}$ and $EV1_{L488}$ were imaged with TEM to evaluate the intactness of the virus after pH change and labeling. When the pH of EV1 was increased to 9.0 several pentamers were detected (red circle). Scale bars 500 nm.

4.3 Infectivity of Labeled EV1

The infectivity of purified unlabeled virus, unlabeled virus with different pH (8.3 and 9.0) and labeled viruses was determined with end-point dilution assay (Figure 3). GMK-cells were first grown in 96-well plate for one day, after which the cells were infected the next day. Dilution series of eight parallel dilutions was made and infection was followed for three days, after which the cells were stained. Infected cells detached from the plate, and were consequently washed away after staining. Finally, infectivity was calculated based on dyed and non-dyed wells.

Infectivity of purified, unlabeled EV1 was high for all three batches. It was also noticed that increasing the pH either to 8.3 or 9.0 did not affect the infectivity of EV1. However, the infectivity was lowered when EV1 was labeled. Lower infectivity was obtained when dye-to-protein ratio was both 37:1 and 10:1. The aim was to preserve the infectivity of EV1, so the last labeling was carried out with even lower amount of dye, with dye-to-protein ratio 5:1. Based on the end-point dilution results, lowest amount of dye (5:1) preserved the infectivity of the virus, higher amount of dye lowered the infectivity by a factor of 10^4 or 10^5.

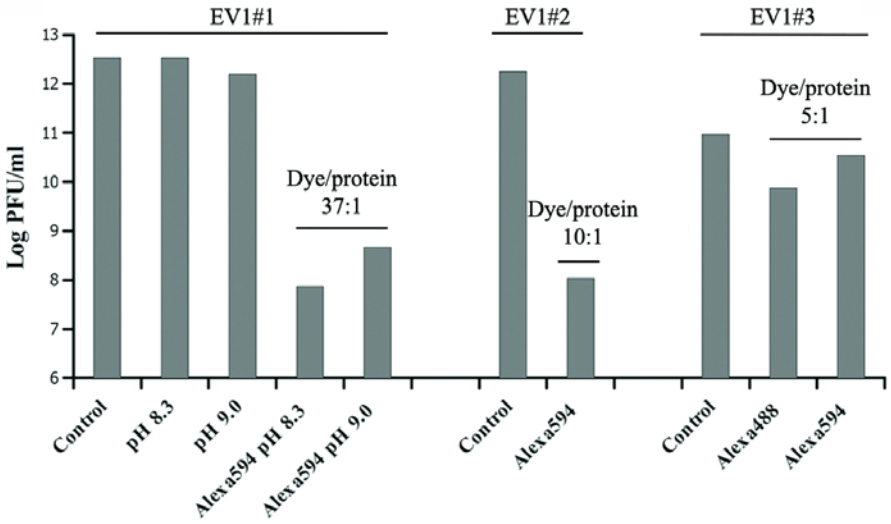

Figure 3. Infectivity of EV1. The infectivity of unlabeled EV1#1, 2 and 3, EV1#1 with higher pH and labeled EV1 (Alexa594 or Alexa488) was determined with end-point dilution assay where dilution series of EV1 with eight parallel dilutions was made. Infection was followed for three days, after which infectivity was calculated (for more details see materials and methods). Three different dye-to-protein ratios were tested: 37:1, 10:1 or 5:1.

4.4 Colocalization of $EV1_{L594}$ with $\alpha_2\beta_1$-Integrin

During the experiments, it was noticed that $EV1_{L594}$ tended to attach to surfaces and was found to be sticky. For that reason, it was valid to test whether $EV1_{L594}$ still attaches to its receptor $\alpha_2\beta_1$-integrin efficiently. Immunofluorescence studies were carried out with two different cell lines and colocalization of $EV1_{L594}$ and antibody labeled EV1 with $\alpha_2\beta_1$-integrin were compared (Figure 4A). Also two different antibodies against $\alpha_2\beta_1$-integrin were compared: a211e10 which competes for binding sites with EV1, and MCA2025 which does not compete with EV1 binding to integrin. Colocalization of EV1 signal with integrin signal was quantified with Bioimage XD softaware (Figure 4B). Colocalization was evaluated from 10 cells from three different experiments.

Quantification results showed, that in SAOS cells, the colocalization of antibody labeled EV1 and $\alpha_2\beta_1$-integrin (48 ± 6%) was lower than the colocalization of $EV1_{L594}$ and $\alpha_2\beta_1$-integrin (65 ± 5%), when a211e10 integrin antibody was used. However, the significance level of this difference was the lowest ($*p < 0.05$). No significant difference ($p > 0.05$) was observed when MCA2025 integrin antibody was used. The colocalization of antibody labeled EV1 and $\alpha_2\beta_1$-integrin was 38 ± 5% and the colocalization of $EV1_{L594}$ and $\alpha_2\beta_1$-integrin was 49 ± 6%. In general, in SAOS cells the colocalization of EV1 and $\alpha_2\beta_1$-integrin was lower when MCA2025 antibody was used, compared to a211e10.

On the other hand, a different result was obtained with A549 cells. When a211e10 anti-integrin was used, no statistically significant difference ($p > 0.05$) was observed between the colocalization of antibody labeled EV1 and $\alpha_2\beta_1$-integrin (59 ± 7%) and the colocalization of $EV1_{L594}$ and $\alpha_2\beta_1$-integrin (51 ± 4%). Instead, when MCA2025 antibody was used, the colocalization of antibody labeled EV1 and $\alpha_2\beta_1$-integrin (62 ± 3%) was significantly higher ($***p < 0.001$) than the colocalization of $EV1_{L594}$ and $\alpha_2\beta_1$-integrin (24 ± 4%).

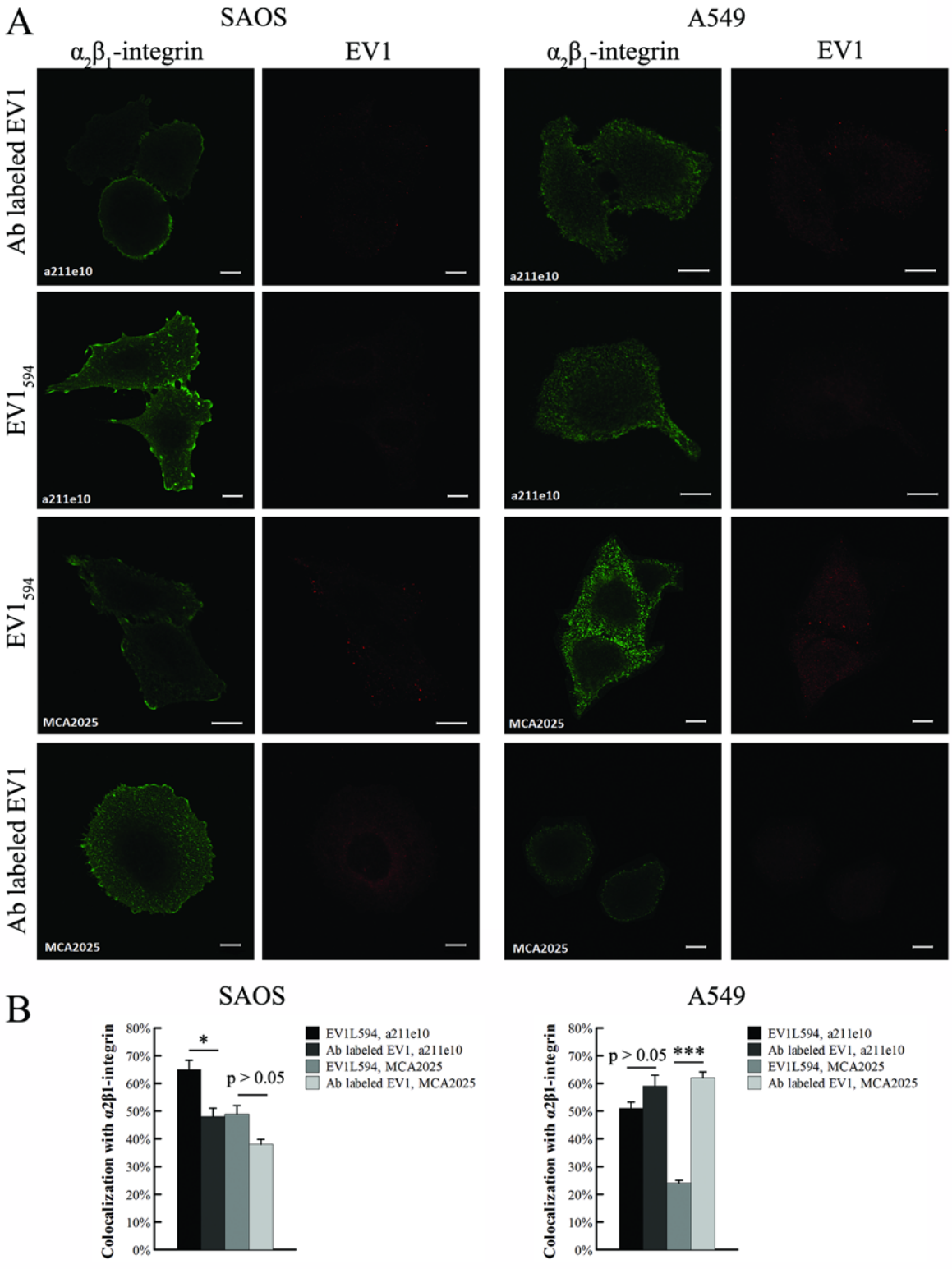

Figure 4. Colocalization of EV1 with its receptor α2β1-integrin. (A) Colocalization of AlexaFluor594 labeled EV1 ($EV1_{L594}$) and antibody labeled EV1 (Ab labeled EV1) with α2β1-integrin in SAOS and A549 cells after 0 h. α2β1-integrin was labeled with either a211e10 or MCA2025 primary antibody and AlexaFluor488 conjugated secondary antibody. EV1 was labeled with anti-EV1 primary antibody and AlexaFluor555 conjugated secondary antibody or with amine reactive dye AlexaFluor594. Scale bars 10µm. (B) Colocalization was quantified with Bioimage XD. The results were counted from three different experiments, 10 cells each.

4.5 Inhibition of EV1 Internalization with U73122

Fluorecently labeled EV1 was used in a study where the aim was to block endocytosis of EV1, and in that way, leave the virus on the cell surface. For this purpose, PLC-inhibitor U73122 was pre-incubated with cells for 30 min before $EV1_{L488}$ infection. After infection, cells were incubated at + 37 °C for 2 h and then fixed. As a control, cells were not treated with U73122 but were fixed and immunolabeled 2 h p.i. In another control, cells were kept and fixed on ice after infection to verify that no internalization would occur (0 h p.i.). After fixation, surface bound EV1 was immunolabeled with anti-EV1 primary antibody and AlexaFluor555 conjugated secondary antibody. Blocking of endocytosis was evaluated by quantifying colocalization of $EV1_{L488}$ with surface labeled EV1. Because EV1 was immunolabeled after fixation without permeabilization, it was assumed that EV1 labeled with antibodies (red signal) would be on the cell surface. The relative amount of $EV1_{L488}$ on the cell surface after two hours could then be evaluated by comparing the signal from $EV1_{L488}$ (green signal) with red signal. On the other hand, green signal that did not colocalize with red signal represented internalized EV1 (Figure 5A). Colocalization was imaged with confocal microscope in two different cell lines: SAOS and A549 cells.

Colocalization was additionally quantified with Bioimage XD (Figure 5B). The colocalization of green signal with red signal was studied in SAOS cells after 0 h when no internalization had occurred (23.69 ± 2.5%). The 0 h time point was compared to the 2 h time point where cells had been treated with U73122 (24.99 ± 3.2%), to see, whether EV1 internalization had been blocked. Results showed no significant increase ($p > 0.05$) in internalization after two hours, when cells were treated with U73122 (Figure 5B, SAOS). Colocalization after 2 h with U73122 treatment was also compared to colocalization after 2 h in cells which were not treated with U73122 (16.47 ± 1.7%). Results showed that colocalization was smaller in cells with no U73122 treatment after 2 h ($*p < 0.05$), indicating that, without U73122, $EV1_{L488}$ had internalized after two hours (Figure 5B, SAOS).

Similar results were obtained with A549 cells (Figure 5B, A549). The colocalization of green signal with red signal was 25.43 ± 3.1% after 0 h and 28.33 ± 2.4% after 2 h with U73122 treatment and no significant difference was detected ($p > 0.05$).

Colocalization after 2 h without U73122 treatment was 21.42 ± 2.0% and was less than with U73122 treatment (*p < 0.05) (Figure 5B, A549). However, in general, the percentage of EV1 on the surface both after zero and two hours was low, under 50 %.

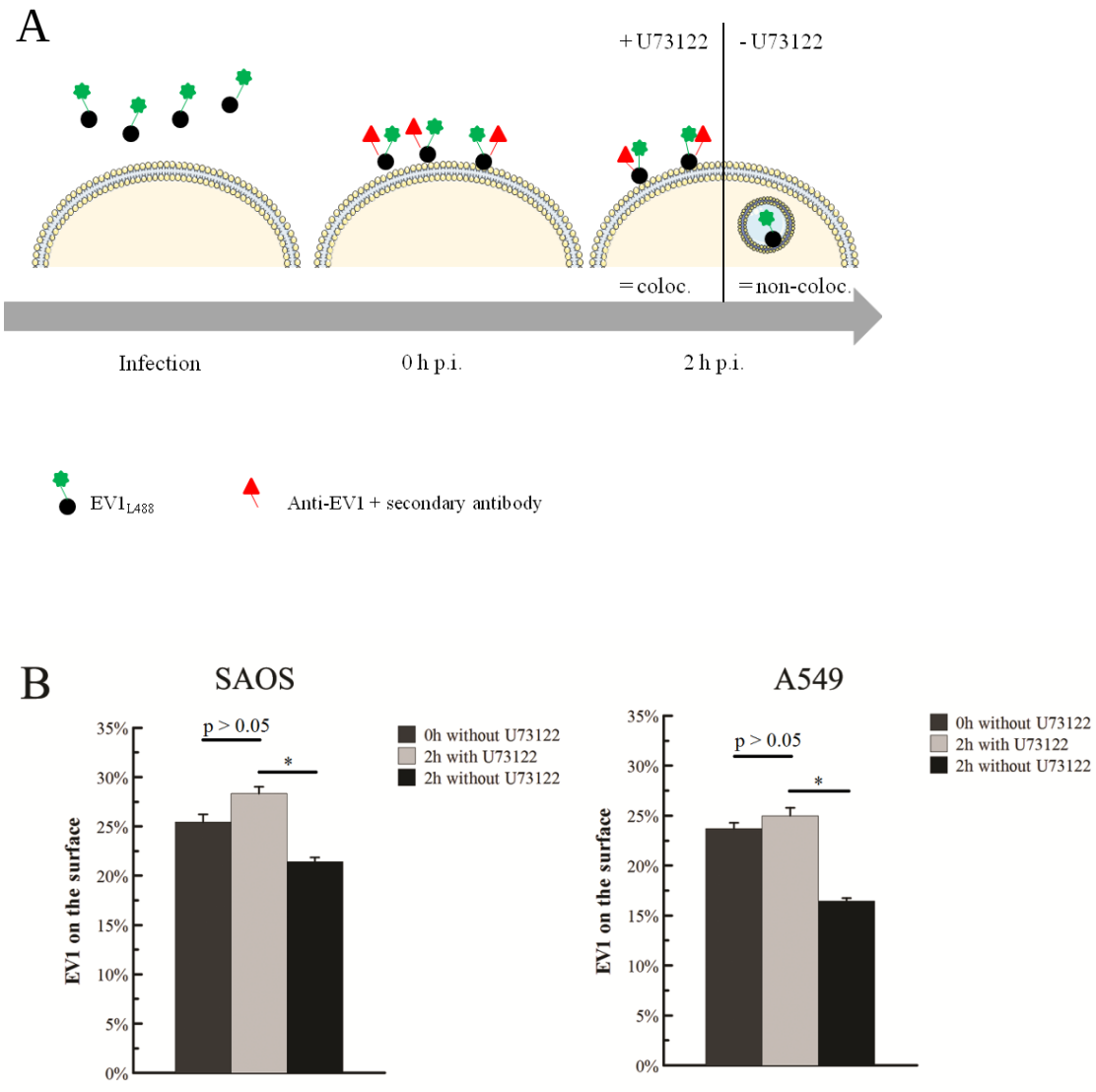

Figure 5. Inhibition of EV1 internalization with U73122. (A) Cells were incubated with U73122 for 30 min before the experiment, and after that, infected with $EV1_{L488}$(green), and labeled after fixation with anti-EV1 primary antibody and AlexaFluor555 conjugated secondary antibody (red). Colocalization of green signal with red signal was studied after 2 h p.i. As a control, cells were not incubated with U73122 and the colocalization of green signal with red signal was studied after 0 h p.i. and 2 h p.i. Green signal colocalizing (coloc.) with the red signal represents EV1 on the surface, and green signal not colocalizing with red (non-coloc.) represents internalized EV1. (B) Colocalization was quantified with Bioimage XD in two cell lines: SAOS and A549. Colocalization of green signal with red signal was counted from three different experiments, 10 cells each.

4.6 EV1 Infection in U73122 Treated Cells

The ability of EV1 to infect was further studied in the presence of U73122. The experiment was carried out with two cell lines SAOS and A549, and cells were first either incubated with U73122 for 30 min or without U73122 before the experiment. After that, cells were infected with $EV1_{L488}$ and after 6 h p.i. labeled with anti-EV1 primary antibody and AlexaFluor555 conjugated secondary antibody. Cells were imaged with confocal microscope and clearly infected cells were found both with and without U73122 in both cell lines (Figure 6A). As a result, 600-800 cells were studied, and infected cells counted. The results showed that the amount of infected cells had decreased, when cells were first treated with U73122 (Figure 6B). The amount of infected SAOS cells without U73122 treatment was 19.8 ± 1.8% and with U73122 treatment 7.7 ± 1.5%, and the results were statistically highly significant (***$p < 0.001$). The results were also statistically significant for A549 cells (**$p < 0.01$) which were infected by 7.2 ± 0.9% without U73122 treatment and by 4.4 ± 0.6%, when treated with U73122. However, the amount of infected A549 cells was lower compared to the SAOS cells. In general, the amount of infected cells was low in both cell lines which might indicate that $EV1_{L488}$ does not infect efficiently.

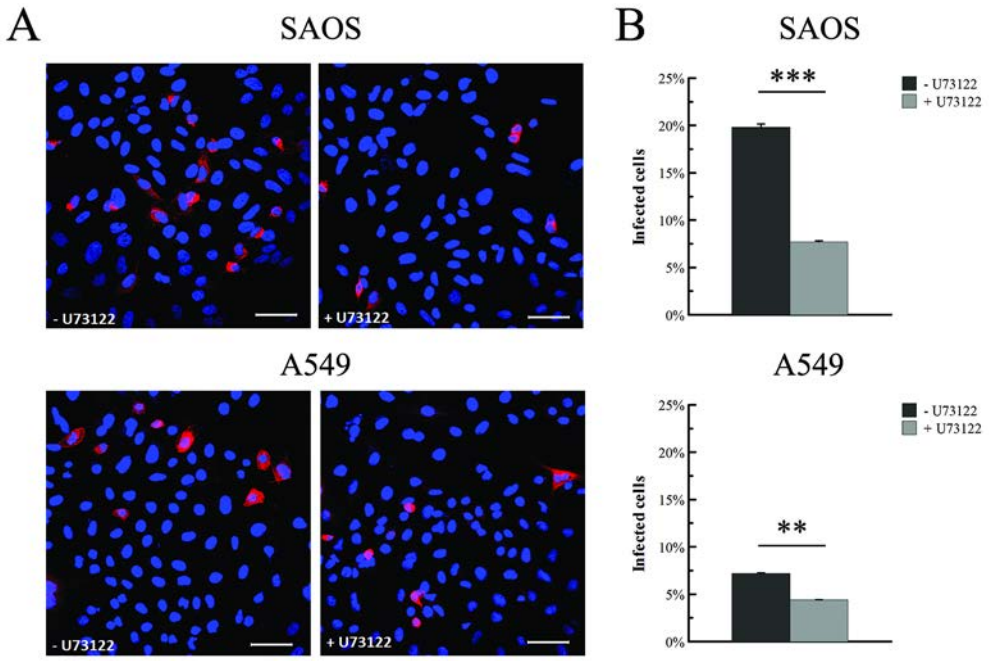

Figure 6. EV1 infection in U73122 treated cells. Cells were first pre-incubated with U73122 for 30 min before experiment (+U73122) or without U73122 (-U73122). Cells were next infected with $EV1_{L488}$ and after 6 h p.i. cells were labeled with anti-EV1 primary antibody and AlexaFluor555 conjugated secondary antibody. Two cell lines SAOS and A549 were studied. (A) Nuclei and infected cells are shown in a merged image. Scale bars 50μm. (B) Based on confocal images, the number of infected cells was quantified as described in materials and methods. 600-800 cells per each sample were checked.

5 Discussion

EV1 is a human pathogen and a member of the *Picornaviridae* family. Studies of the early steps of EV1 infection have shown that, EV1 binds to $\alpha_2\beta_1$-integrin (Bergelson et al., 1992) and is then endocytoced by a mechanism that resembles both caveolin-mediated endocytosis and macropinocytosis (Marjomaki et al., 2002; Karjalainen et al., 2008). However, the mechanism by which EV1 and other picornaviruses deliver their genome is poorly understood. Uncoating studies are hindered by difficulties related to direct visualization of genome delivery. Here, we have purified EV1 and fluorescently labeled the virus capsid with an amine reactive dye. Fluorescent capsid label provides us a tool for future uncoating and live imaging studies, where EV1 can be tracked directly and non-specificity that is usually related to immunolabeling is minimized. The technique is widely used and fluorescent labeling of both the envelope of enveloped viruses and capsid of non-enveloped viruses has been carried out previously, when viral lifecycle in living cells has been studied (Brandenburg et al., 2007; Pelkmans et al., 2001; Lakadamyali et al., 2003; Campbell and Hope, 2008).

EV1 was purified with sucrose gradient to obtain intact and infectious particles for labeling. In three purifications, EV1 was successfully separated from cellular material even though, the virus was found from different fraction each time in the gradient. The gradients were prepared manually which might have caused the difference in virus location. More empty and disassembled particles were detected in EV1#3 batch, which might be because the virus band was higher in the gradient than what has been typically observed earlier. Empty and disassembled particles are lighter than intact particles and are located higher in the gradient. In EV1#3, virus band was also higher and as a result, also more empty and disassembled particles were collected in addition to intact particles. Optimal labeling was hindered by dye attaching to empty and disassembled particles, and as a result, additionally false signal was probably detected in immunofluorescence studies. Normally, empty and disassembled particles are washed away during immunolabeling, but now, hydrophopic dye might have allowed those particles to be present as well.

EV1 infectivity was noticed to suffer from fluorescent labeling of the capsid. The infectivity was lowered the most when higher dye-to-protein ratios (37:1 and 10:1) were used. The lowest dye-to-protein ratio (5:1) decreased the infectivity marginally and after three different labeling, this considerably low amount of dye was found sufficient for signal detection, and more importantly, was found necessary for maintaining virus infectivity. To verify that lower infectivity was due to labeling, and not pH change, the infectivity of EV1 with higher pH without labeling was tested. The results showed no change in infectivity due to pH change alone. The results also showed that pH 8.3 is high enough for successful labeling, and for that reason, second and third labeling was carried out with pH 8.3 instead of pH 9.0. In addition, pH 9.0 was observed to break up the virus particles more, which was assessed by detection of pentamers with TEM. Some of the virus particles are always disassembled even at pH 7.0 and hence, viruses are partially broken down into pentamers, but when pH was increased to 9.0, clearly more pentamers were observed. When pH was increased to 8.3, pentameric structures were not abundant, indicating that the degradation was more likely due to increased pH and not labeling.

After EV1 was fluorescently labeled, the degree of labeling was determined spectrophotometrically. The target for labeling is mostly primary amines of lysine residues, and based on EV1 sequence, the theoretical degree of labeling was assumed to be less than 1380 (UniprotKB ID: O91734). This assumption was supported by our results, when the degree of labeling was around 100-500 fluorophores per particle. However, the degree of labeling was highest in EV1#3 where dye-to-protein ratio was the lowest. The difference between the first two batches and the third batch was that EV1#3 contained more disassembled and empty particles where lysine residues may have been more accessible than in intact particles, which might have increased the degree of labeling. Degree of labeling cannot be attributed to only intact particles, but instead, all the dye that is present in the sample is included in the calculations. Consequently, more optimization is needed in terms of EV1 purity before labeling.

During EV1 labeling, it was noticed that the dye is hydrophopic and therefore $EV1_{L594}$ tended to attach to the surfaces. Consequently, colocalization of $EV1_{L594}$ and antibody labeled EV1 with $\alpha_2\beta_1$-integrin was quantified and compared to verify that $EV1_{L594}$ still specifically binds to its receptor $\alpha_2\beta_1$-integrin instead of non-specifically on the cell

surface. The experiment was carried out with two different cell lines, SAOS and A549 cells, which express different levels of $\alpha_2\beta_1$-integrin, and different results were obtained between the two cell lines. In SAOS cells, the colocalization of $EV1_{L594}$ with $\alpha_2\beta_1$-integrin was higher than the colocalization of antibody labeled EV1 with $\alpha_2\beta_1$-integrin, when a211e10 anti-integrin antibody was used. On the other hand, when MCA2025 anti-integrin was used, no statistically significant difference was observed. In A549 cells however, the colocalization of $EV1_{L594}$ with $\alpha_2\beta_1$-integrin was not significantly different from the colocalization of antibody labeled EV1 with $\alpha_2\beta_1$-integrin, when a211e10 anti-integrin antibody was used. Instead, statistically significant difference was found when MCA2025 anti-integrin antibody was used. The colocalization of $EV1_{L594}$ with $\alpha_2\beta_1$-integrin was lower than the colocalization of antibody labeled EV1 with $\alpha_2\beta_1$-integrin, when MCA2025 antibody was used. Consequently, no clear trend could be found when comparing the colocalizations, which might be due to antibody aggregates that were observed in confocal images. Normally after 0 h, EV1 is not observed as bright clusters but instead the signal should be more diffused. However, bright big clusters were detected during confocal studies and it was suspected that they were antibody aggregates.

According to the $\alpha_2\beta_1$-integrin colocalization results, only ~50% of EV1 was observed to bind its receptor, which is contradictory with the assumption that the virus binds specifically and efficiently to its receptor on a host cell, and starts infection. Instead, based on our results, the remaining half is somewhere else on the surface than bound to $\alpha_2\beta_1$-integrin. But because our antibody was probably aggregated, it cannot be confirmed with our results whether the phenomenon is real or not. In addition, the 0 h time point might not be the most optimal to tell the relationship between EV1 and its receptor, since the virus have not had time to cluster $\alpha_2\beta_1$-integrin on the cell surface (Jokinen et al., 2010). It has been shown previously that EV1 binds to $\alpha_2\beta_1$-integrin on the cell surface and both EV1 and $\alpha_2\beta_1$-integrin are later found in cytoplasmic vesicles which grow in size and localize closer to the cell center during time (Karjalainen et al., 2011). Based on the results showed by Karjalainen et al. in 2011, 5-10 min time point could have been more informative about EV1 colocalizing with $\alpha_2\beta_1$-integrin, since EV1 would have had time to cluster $\alpha_2\beta_1$-integrin. Additionally, it cannot be ruled out that EV1 probably has undergone changes over the years during serial passages, which might also affect the colocalization with $\alpha_2\beta_1$-integrin. However, more studies are needed to verify that EV1 has changed during

passages, and no conclusions can be drawn based on our studies and results. On the other hand, even though it has been shown that $\alpha_2\beta_1$-integrin is the receptor for EV1, it is also known that, in addition to their main receptor, viruses might also use other molecules during their entry. For EV1, it has been shown that, in addition to $\alpha_2\beta_1$-integrin, at least β_2 microglobulin affects the entry of the virus, since the internalization is inhibited by antibodies against β_2 microglobulin (Marjomaki et al., 2002; Ward et al., 1998).

In addition to EV1 labeling, future uncoating studies were considered in an experiment, where the aim was to block EV1 internalization, and as a result, leave the virus on the cell surface. Uncoating most probably takes place inside endosomal structures, which are challenging environments to be studied. Accordingly, we intended to create a system, where EV1 uncoating could be controlled and studied on the cell surface, instead of inside endosomes. As a result, PLC-inhibitor U73122 was tested as an endocytosis blocker and our results showed that EV1 internalization was blocked by U73122. This is consistent with previous results showed by Karjalainen et al. in 2008. However, the amount of EV1 on the surface was low in general, since also the amount of EV1 on the surface in control cells after 0 h was under 50%. In addition, although a statistically significant difference was obtained in 2 h samples between U73122 treated and untreated cells, the difference was only 10%.

Internalization study was carried out with fluorescently labeled $EV1_{L488}$. The study was hindered by false signal that probably originated from fluorescently labeled empty and disassembled virus particles and aggregates, which were not washed away probably because of the hydrophobicity of the dye. In addition, large amount of dye might have prevented proper binding of antibody to $EV1_{L488}$, and as a result, colocalization is not as substantial. Green signal, not colocalizing with red signal, should represent internalized EV1, but here it could also represent EV1, which has been covered with Alexa488 capsid label, and do not have binding sites for antibody. This could also explain why colocalization is low in control cells after 0 h. On the other hand, red signal not colocalizing with green signal, could represent virus particles, which have not been labeled at all with the fluorescent capsid label Alexa488, but are labeled with anti-EV1 primary antibody and AlexaFluor555 conjugated secondary antibody. The colocalization of green signal with red signal was quantified here, not vice versa, but because spots of red signal

not colocalizing with green signal were also detected in the confocal images (data not shown), it can be additionally deduced that not all virus particles were labeled.

Fluorescently labeled EV1 was also used in an experiment, where EV1 infection was further studied in the presence of U73122. Infected cells were found both in the presence of U73122 and with no U73122, and also less infected cells were detected in both cases. Even though the number of infected cells was decreased in the presence of U73122, there still were several infected cells, and so the leakage of virus from the cell surface was evident. Our results are not consistent with what have been shown previously, since the results by Karjalainen et al., in 2008, indicated that EV1 infection is totally blocked, when cells are treated with U73122 for 30 min before the experiment. Our results showed a decrease in infection but around 5% of the cells were still infected. This may arise partially from the variation in the solubility and/or stability of the drug that is dissolved in dimethylsulphoxide and stored at -80 °C. Thus, the functionality of U73122 still needs to be studied more and verify.

These experiments were also hampered by low infectivity of control cells, which were infected by only ~20% (SAOS) or ~7% (A549). Low infectivity in control cells could indicate that $EV1_{L488}$ still does not infect efficiently, and labeling has to be more optimized. Although according to end-point dilution results, $EV1_{L488}$ infectivity was preserved, the results might tell that the infectivity was good enough to start the infection. In the end-point dilution assay, the infection was followed for three days, and in that time, a lot of new virus particles were formed and fully infected cells had freed new particles (without the label), which could infect other cells. Instead, in the 6 h p.i. experiment, the infection time is only 6 h, and by that time, not that many cells are fully infected and have freed new particles to infect other cells. So as a result, $EV1_{L488}$ infectivity might, in that sense, have been weaker than what end-point dilution assay indicated. In addition, it might be that more viruses would have been needed to infect the cells, since the concentration was low, and not all viruses were infectious.

During the studies, also a question arose whether EV1 could translocate its genome into the cytoplasm, and start infection even when left on the cell surface. It has been shown that poliovirus relies on endocytosis during infection, which disproved earlier speculations, where the virus was thought to be able to infect directly through plasma membrane

(Brandenburg et al., 2007). However, with our system we could study whether EV1 could translocate its genome through plasma membrane, when forced to stay on the cell surface. Our hypothesis was that infection would not be as evident after 6 h p.i. as without U73122, but instead, would start slower. If EV1 could infect from the cell surface, it could be further speculated whether endocytosis is actually needed for infection or if it is a side effect that just occurs even though it is not necessary. However, based on our studies and results, the ability of EV1 to infect from the cell surface through plasma membrane, could not be reliably verified. The possibility of slower infection could not be evaluated by studying different populations of infected cells, since the difference between the leakage of the virus and slow infection could not be separated. Consequently, before further studies regarding EV1 infection from the cell surface, the functionality of U73122 has to be verified.

In conclusion, the main focus of this thesis was to lay foundation for the future uncoating studies in vitro. Therefore, EV1 capsid was labeled with a fluorescent dye to acquire a tool for visualization and tracking of EV1 in cells. The advantage of this technique is a permanent attachment of the dye by covalent binding and minimization of background due to unspecific binding of antibodies. On the other hand, efficient labeling with low background was found to be dependent on the purity of the virus since empty and disassembled particles were also labeled. In addition, fluorescent labeling of EV1 capsid affected the infectivity of the virus, and the right degree of labeling for sufficient signal and preserved infectivity had to be optimized. According to our results, more optimization is needed for efficient labeling so that non-intact virions, which both cause background and lower the infectivity, are eliminated.

Fluorescently labeled EV1 was also used in cellular experiments, where the purpose was to leave EV1 on the cell surface by blocking endocytosis. If succeeded, EV1 uncoating could be studied on the cell surface instead of endosomes. PLC-inhibitor U73122 was used to inhibit internalization, and our results showed a minor blocking effect but, in addition, leakage of virus from the cell surface was evident. Thus, the functionality of U73122 needs to be studied more in the future and verify before use in the uncoating studies.

6 References

Arnaout, M.A., B. Mahalingam, and J.P. Xiong. 2005. Integrin structure, allostery, and bidirectional signaling. *Annu.Rev.Cell Dev.Biol.* 21:381-410.

Bayer, N., D. Schober, E. Prchla, R.F. Murphy, D. Blaas, and R. Fuchs. 1998. Effect of bafilomycin A1 and nocodazole on endocytic transport in HeLa cells: implications for viral uncoating and infection. *J.Virol.* 72:9645-9655.

Belnap, D.M., D.J. Filman, B.L. Trus, N. Cheng, F.P. Booy, J.F. Conway, S. Curry, C.N. Hiremath, S.K. Tsang, A.C. Steven, and J.M. Hogle. 2000. Molecular tectonic model of virus structural transitions: the putative cell entry states of poliovirus. *J.Virol.* 74:1342-1354.

Bergelson, J.M., B.M. Chan, R.W. Finberg, and M.E. Hemler. 1993. The integrin VLA-2 binds echovirus 1 and extracellular matrix ligands by different mechanisms. *J.Clin.Invest.* 92:232-239.

Bergelson, J.M., J.A. Cunningham, G. Droguett, E.A. Kurt-Jones, A. Krithivas, J.S. Hong, M.S. Horwitz, R.L. Crowell, and R.W. Finberg. 1997. Isolation of a common receptor for Coxsackie B viruses and adenoviruses 2 and 5. *Science.* 275:1320-1323.

Bergelson, J.M., M.P. Shepley, B.M. Chan, M.E. Hemler, and R.W. Finberg. 1992. Identification of the integrin VLA-2 as a receptor for echovirus 1. *Science.* 255:1718-1720.

Berinstein, A., M. Roivainen, T. Hovi, P.W. Mason, and B. Baxt. 1995. Antibodies to the vitronectin receptor (integrin alpha V beta 3) inhibit binding and infection of foot-and-mouth disease virus to cultured cells. *J.Virol.* 69:2664-2666.

Berryman, S., S. Clark, P. Monaghan, and T. Jackson. 2005. Early events in integrin alphavbeta6-mediated cell entry of foot-and-mouth disease virus. *J.Virol.* 79:8519-8534.

Bishop, N.E. 1998. Examination of potential inhibitors of hepatitis A virus uncoating. *Intervirology.* 41:261-271.

Bostina, M., H. Levy, D.J. Filman, and J.M. Hogle. 2011. Poliovirus RNA is released from the capsid near a twofold symmetry axis. *J.Virol.* 85:776-783.

Brandenburg, B., L.Y. Lee, M. Lakadamyali, M.J. Rust, X. Zhuang, and J.M. Hogle. 2007. Imaging poliovirus entry in live cells. *PLoS Biol.* 5:e183.

Campbell, E.M., and T.J. Hope. 2008. Live cell imaging of the HIV-1 life cycle. *Trends Microbiol.* 16:580-587.

Connors, W.L., J. Jokinen, D.J. White, J.S. Puranen, P. Kankaanpaa, P. Upla, M. Tulla, M.S. Johnson, and J. Heino. 2007. Two synergistic activation mechanisms of alpha2beta1 integrin-mediated collagen binding. *J.Biol.Chem.* 282:14675-14683.

Coyne, C.B., and J.M. Bergelson. 2006. Virus-induced Abl and Fyn kinase signals permit coxsackievirus entry through epithelial tight junctions. *Cell.* 124:119-131.

Curry, S., M. Chow, and J.M. Hogle. 1996. The poliovirus 135S particle is infectious. *J.Virol.* 70:7125-7131.

Fricks, C.E., and J.M. Hogle. 1990. Cell-induced conformational change in poliovirus: externalization of the amino terminus of VP1 is responsible for liposome binding. *J.Virol.* 64:1934-1945.

Fuchs, R., and D. Blaas. 2012. Productive entry pathways of human rhinoviruses. *Adv.Virol.* 2012:826301.

Greve, J.M., G. Davis, A.M. Meyer, C.P. Forte, S.C. Yost, C.W. Marlor, M.E. Kamarck, and A. McClelland. 1989. The major human rhinovirus receptor is ICAM-1. *Cell.* 56:839-847.

Grunert, H.P., K.U. Wolf, K.D. Langner, D. Sawitzky, K.O. Habermehl, and H. Zeichhardt. 1997. Internalization of human rhinovirus 14 into HeLa and ICAM-1-transfected BHK cells. *Med.Microbiol.Immunol.* 186:1-9.

Hadfield, A.T., W. Lee, R. Zhao, M.A. Oliveira, I. Minor, R.R. Rueckert, and M.G. Rossmann. 1997. The refined structure of human rhinovirus 16 at 2.15 A resolution: implications for the viral life cycle. *Structure.* 5:427-441.

Harutyunyan, S., M. Kumar, A. Sedivy, X. Subirats, H. Kowalski, G. Kohler, and D. Blaas. 2013. Viral uncoating is directional: exit of the genomic RNA in a common cold virus starts with the poly-(A) tail at the 3'-end. *PLoS Pathog.* 9:e1003270.

Hofer, F., M. Gruenberger, H. Kowalski, H. Machat, M. Huettinger, E. Kuechler, and D. Blaas. 1994. Members of the low density lipoprotein receptor family mediate cell entry of a minor-group common cold virus. *Proc.Natl.Acad.Sci.U.S.A.* 91:1839-1842.

Hughes, P.J., C. Horsnell, T. Hyypia, and G. Stanway. 1995. The coxsackievirus A9 RGD motif is not essential for virus viability. *J.Virol.* 69:8035-8040.

Huttunen, M., M. Waris, R. Kajander, T. Hyypia, and V. Marjomaki. 2014. Coxsackievirus A9 Infects Cells via Non-acidic Multivesicular Bodies. *J.Virol.*

Hynes, R.O. 2002. Integrins: bidirectional, allosteric signaling machines. *Cell.* 110:673-687.

Jackson, T., F.M. Ellard, R.A. Ghazaleh, S.M. Brookes, W.E. Blakemore, A.H. Corteyn, D.I. Stuart, J.W. Newman, and A.M. King. 1996. Efficient infection of cells in culture by type O foot-and-mouth disease virus requires binding to cell surface heparan sulfate. *J.Virol.* 70:5282-5287.

Jackson, T., D. Sheppard, M. Denyer, W. Blakemore, and A.M. King. 2000. The epithelial integrin alphavbeta6 is a receptor for foot-and-mouth disease virus. *J.Virol.* 74:4949-4956.

Jokinen, J., D.J. White, M. Salmela, M. Huhtala, J. Kapyla, K. Sipila, J.S. Puranen, L. Nissinen, P. Kankaanpaa, V. Marjomaki, T. Hyypia, M.S. Johnson, and J. Heino. 2010. Molecular mechanism of alpha2beta1 integrin interaction with human echovirus 1. *EMBO J.* 29:196-208.

Kankaanpaa, P., L. Paavolainen, S. Tiitta, M. Karjalainen, J. Paivarinne, J. Nieminen, V. Marjomaki, J. Heino, and D.J. White. 2012. BioImageXD: an open, general-purpose and high-throughput image-processing platform. *Nat.Methods.* 9:683-689.

Kaplan, G., M.S. Freistadt, and V.R. Racaniello. 1990. Neutralization of poliovirus by cell receptors expressed in insect cells. *J.Virol.* 64:4697-4702.

Kaplan, G., A. Totsuka, P. Thompson, T. Akatsuka, Y. Moritsugu, and S.M. Feinstone. 1996. Identification of a surface glycoprotein on African green monkey kidney cells as a receptor for hepatitis A virus. *EMBO J.* 15:4282-4296.

Karjalainen, M., E. Kakkonen, P. Upla, H. Paloranta, P. Kankaanpaa, P. Liberali, G.H. Renkema, T. Hyypia, J. Heino, and V. Marjomaki. 2008. A Raft-derived, Pak1-regulated entry participates in alpha2beta1 integrin-dependent sorting to caveosomes. *Mol.Biol.Cell.* 19:2857-2869.

Karjalainen, M., N. Rintanen, M. Lehkonen, K. Kallio, A. Maki, K. Hellstrom, V. Siljamaki, P. Upla, and V. Marjomaki. 2011. Echovirus 1 infection depends on biogenesis of novel multivesicular bodies. *Cell.Microbiol.*13:1975-1995.

Khan, A.G., A. Pickl-Herk, L. Gajdzik, T.C. Marlovits, R. Fuchs, and D. Blaas. 2010. Human rhinovirus 14 enters rhabdomyosarcoma cells expressing icam-1 by a clathrin-, caveolin-, and flotillin-independent pathway. *J.Virol.* 84:3984-3992.

King, S.L., J.A. Cunningham, R.W. Finberg, and J.M. Bergelson. 1995. Echovirus 1 interaction with the isolated VLA-2 I domain. *J.Virol.* 69:3237-3239.

Kotaniemi-Syrjanen, A., R. Vainionpaa, T.M. Reijonen, M. Waris, K. Korhonen, and M. Korppi. 2003. Rhinovirus-induced wheezing in infancy--the first sign of childhood asthma? *J.Allergy Clin.Immunol.* 111:66-71.

Lakadamyali, M., M.J. Rust, H.P. Babcock, and X. Zhuang. 2003. Visualizing infection of individual influenza viruses. *Proc.Natl.Acad.Sci.U.S.A.* 100:9280-9285.

Levy, H.C., M. Bostina, D.J. Filman, and J.M. Hogle. 2010. Catching a virus in the act of RNA release: a novel poliovirus uncoating intermediate characterized by cryo-electron microscopy. *J.Virol.* 84:4426-4441.

Lyu, K., J. Ding, J.F. Han, Y. Zhang, X.Y. Wu, Y.L. He, C.F. Qin, and R. Chen. 2014. Human enterovirus 71 uncoating captured at atomic resolution. *J.Virol.* 88:3114-3126.

Marjomaki, V., V. Pietiainen, H. Matilainen, P. Upla, J. Ivaska, L. Nissinen, H. Reunanen, P. Huttunen, T. Hyypia, and J. Heino. 2002. Internalization of echovirus 1 in caveolae. *J.Virol.* 76:1856-1865.

Martinez, M.A., N. Verdaguer, M.G. Mateu, and E. Domingo. 1997. Evolution subverting essentiality: dispensability of the cell attachment Arg-Gly-Asp motif in multiply passaged foot-and-mouth disease virus. *Proc.Natl.Acad.Sci.U.S.A.* 94:6798-6802.

Mendelsohn, C.L., E. Wimmer, and V.R. Racaniello. 1989. Cellular receptor for poliovirus: molecular cloning, nucleotide sequence, and expression of a new member of the immunoglobulin superfamily. *Cell.* 56:855-865.

Oberste, M.S., and M.A. Pallansch. 2003. Establishing evidence for enterovirus infection in chronic disease. *Ann.N.Y.Acad.Sci.* 1005:23-31.

Parton, R.G. 1996. Caveolae and caveolins. *Curr.Opin.Cell Biol.* 8:542-548.

Pelkmans, L., J. Kartenbeck, and A. Helenius. 2001. Caveolar endocytosis of simian virus 40 reveals a new two-step vesicular-transport pathway to the ER. *Nat.Cell Biol.* 3:473-483.

Pierschbacher, M.D., and E. Ruoslahti. 1984. Variants of the cell recognition site of fibronectin that retain attachment-promoting activity. *Proc.Natl.Acad.Sci.U.S.A.* 81:5985-5988.

Pietiainen, V., V. Marjomaki, P. Upla, L. Pelkmans, A. Helenius, and T. Hyypia. 2004. Echovirus 1 endocytosis into caveosomes requires lipid rafts, dynamin II, and signaling events. *Mol.Biol.Cell.* 15:4911-4925.

Quest, A.F., L. Leyton, and M. Parraga. 2004. Caveolins, caveolae, and lipid rafts in cellular transport, signaling, and disease. *Biochem.Cell Biol.* 82:129-144.

Reischl, A., M. Reithmayer, G. Winsauer, R. Moser, I. Gosler, and D. Blaas. 2001. Viral evolution toward change in receptor usage: adaptation of a major group human rhinovirus to grow in ICAM-1-negative cells. *J.Virol.* 75:9312-9319.

Ren, J., X. Wang, Z. Hu, Q. Gao, Y. Sun, X. Li, C. Porta, T.S. Walter, R.J. Gilbert, Y. Zhao, D. Axford, M. Williams, K. McAuley, D.J. Rowlands, W. Yin, J. Wang, D.I. Stuart, Z. Rao, and E.E. Fry. 2013. Picornavirus uncoating intermediate captured in atomic detail. *Nat.Commun.* 4:1929.

Rossmann, M.G., J. Bella, P.R. Kolatkar, Y. He, E. Wimmer, R.J. Kuhn, and T.S. Baker. 2000. Cell recognition and entry by rhino- and enteroviruses. *Virology.* 269:239-247.

Rossmann, M.G., Y. He, and R.J. Kuhn. 2002. Picornavirus-receptor interactions. *Trends Microbiol.* 10:324-331.

Shafren, D.R., D.J. Dorahy, S.J. Greive, G.F. Burns, and R.D. Barry. 1997a. Mouse cells expressing human intercellular adhesion molecule-1 are susceptible to infection by coxsackievirus A21. *J.Virol.* 71:785-789.

Shafren, D.R., D.J. Dorahy, R.A. Ingham, G.F. Burns, and R.D. Barry. 1997b. Coxsackievirus A21 binds to decay-accelerating factor but requires intercellular adhesion molecule 1 for cell entry. *J.Virol.* 71:4736-4743.

Shafren, D.R., D.J. Dorahy, R.A. Ingham, G.F. Burns, and R.D. Barry. 1997c. Coxsackievirus A21 binds to decay-accelerating factor but requires intercellular adhesion molecule 1 for cell entry. *J.Virol.* 71:4736-4743.

Shafren, D.R., D.T. Williams, and R.D. Barry. 1997d. A decay-accelerating factor-binding strain of coxsackievirus B3 requires the coxsackievirus-adenovirus receptor protein to mediate lytic infection of rhabdomyosarcoma cells. *J.Virol.* 71:9844-9848.

Ward, T., R.M. Powell, P.A. Pipkin, D.J. Evans, P.D. Minor, and J.W. Almond. 1998. Role for beta2-microglobulin in echovirus infection of rhabdomyosarcoma cells. *J.Virol.* 72:5360-5365.

Xing, L., M. Huhtala, V. Pietiainen, J. Kapyla, K. Vuorinen, V. Marjomaki, J. Heino, M.S. Johnson, T. Hyypia, and R.H. Cheng. 2004. Structural and functional analysis of integrin alpha2I domain interaction with echovirus 1. *J.Biol.Chem.* 279:11632-11638.

Zhou, L., Y. Luo, Y. Wu, J. Tsao, and M. Luo. 2000. Sialylation of the host receptor may modulate entry of demyelinating persistent Theiler's virus. *J.Virol.* 74:1477-1485.